
SYNCHRONOUS MACHINE FIELD CURRENT CALCULATION TAKING INTO ACCOUNT THE MAGNETIC SATURATION

Ernesto Ruppert Filho*
ruppert@fee.unicamp.br

Francisco Liszt Nunes Jr.*

Sidney Osses Nunes*

* Systems and Energy Control Department - Computer and Electrical Engineering School – Campinas University, DSCE-FEEC-UNICAMP, P.O. Box: 6101, CEP: 13081-970 Campinas-SP-Brasil

ABSTRACT

A synchronous machine dynamic mathematical model including the saturation effect is presented. The saturation modeling deals with the linkage flux mathematical model and uses the machine d-axis and q-axis magnetizing curves. Results are shown in the form of V curves and comparisons with calculations using non-saturated and saturated reactances are done showing a considerable difference in the excitation current values. Comparisons with experimental data are done.

KEYWORDS: Synchronous machine, dynamic model, saturation model, magnetic saturation.

1 INTRODUCTION

Synchronous machines are intensively used as generators due to its very good voltage and frequency regulation characteristics. To study the control of the generated real and reactive power it is necessary to have a very accurate mathematical dynamic model to implement efficient simulations.

A synchronous generator, connected to an infinite bus which voltage is the generator rated voltage, has its stable operating point defined by the following rated val-

ues: armature voltage, apparent power, speed, power factor and excitation voltage. This set of values defines the load angle, armature winding current and excitation current.

In general, due to economic reason, the synchronous generator operates in the saturated part of the magnetizing curve so that the variables are very sensitive to load and excitation current variations. So it is necessary to include magnetic saturation effects in the generator mathematical model to make it more accurate to represent the machine both in transient and steady-state operation.

The magnetic saturation plays an important role in the definition of the excitation current required for the generator operation when producing very well defined real and reactive power, that is, generator operating with a very well defined real power and power factor since it is fed by the rated bus voltage and driven by a mechanical torque corresponding to its real power (load).

The excitation current is very important to power system engineers for electrical energy system generators stability calculation initialization. The most realistic value of the excitation current is also very important to the excitation system design.

For these very reasons it is important that all the electrical energy system stability calculations, using simula-

Artigo submetido em 18/12/00

1a. Revisão em 16/05/01; 2a. Revisão 21/02/02

Aceito sob recomendação do Ed. Assoc. Prof. Denizar C. Martins

tion, include the saturation effects in the mathematical dynamic model.

Several methods to represent the magnetic saturation in synchronous machines have been presented in the literature like [1, 2, 3, 4] dealing, in general, with modifications in the d-axis and q-axis reactance. Generator manufacturers use to provide the machine d-axis and q-axis synchronous non-saturated and saturated reactance to the utility customers. These reactance are frequently used by the electrical energy system engineers to carry transient stability studies, system stability for small disturbances and other types of studies that depend fundamentally from generator variable values at the instant of a disturbance occurrence.

In this paper it is presented a generator dynamic mathematical model where the differential equations are written in terms of the d-axis and q-axis stator and rotor winding linkage fluxes and currents as seen in [5], including a sub model of magnetic saturation in the iron (saturation in the air is not considered) involving the d-axis and q-axis generator magnetizing curves.

In spite of the model be a dynamic model, in this paper it is presented only steady-state simulation results through the generator V curves obtained using non-saturated reactance, saturated reactance and the model mentioned above. The results for an hydrogenerator, which data are in the appendix, are compared and commented.

2 SYNCHRONOUS MACHINE MATHEMATICAL DYNAMIC MODEL

A dynamic mathematical model of a synchronous machine operating as a generator is shown below [5]:

$$\begin{aligned}
 v_q &= -r_s i_q + \frac{\omega_r}{\omega_b} \Psi_d + \frac{p}{\omega_b} \Psi_q, \\
 v_d &= -r_s i_d - \frac{\omega_r}{\omega_b} \Psi_q + \frac{p}{\omega_b} \Psi_d, \\
 v_o &= -r_s i_o + \frac{p}{\omega_b} \Psi_o, & p\theta_r &= \omega_r, \\
 0 &= r_{aq} i_{aq} + \frac{p}{\omega_b} \Psi_{aq}, & p\theta_e &= \omega_e, \\
 v_f &= r_f i_f + \frac{p}{\omega_b} \Psi_f, & \delta &= \theta_r - \theta_e, \\
 0 &= r_{ad} i_{ad} + \frac{p}{\omega_b} \Psi_{ad}, & \omega_m &= \frac{2}{p} \omega_r, \\
 T_e &= \frac{3}{2} \frac{P}{2} \frac{1}{\omega_b} (\Psi_d i_q - \Psi_q i_d), \\
 p\omega_r &= \frac{P}{2J} (T_a - T_e),
 \end{aligned} \tag{1}$$

where: v_d and v_q are the q-axis and d-axis components of the stator winding phase voltage, v_f is the field winding voltage, i_q and i_d are the qd components of the stator winding current, i_f , i_{aq} and i_{ad} are respectively, the field winding, q-axis and d-axis damping winding currents, r_s is the stator winding per phase electrical resistance, r_f , r_{aq} and r_{ad} are the field winding electrical resistance, the q-axis and the d-axis damping winding electrical resistances respectively, ω_r is the rotor electrical angular speed, ω_b is the base electrical angular speed (which is used to calculate reactance), Ψ_q and Ψ_d are the stator winding q and d-axis phase linkage fluxes per second (volts), Ψ_f , Ψ_{aq} and Ψ_{ad} are respectively, the field winding, the q-axis and the d-axis damping winding linkage fluxes per second (volts), p is the differential operator, P is the machine pole number, J is the inertia moment of the machine and turbine rotors, T_a is the driving torque (turbine torque), T_e is the machine electromagnetic torque, θ_r is the angular position of the q-axis referred to the stator winding phase-a magnetic field axis, θ_e is the angular position of the maximum value of the stator winding phase-a voltage, ω_e is the stator winding voltage electrical angular speed (synchronous speed), ω_m is the mechanical angular speed and δ is the load angle of the machine.

The variables with subscript o are the corresponding zero sequence variables that are important when non-balanced studies need to be made.

The linkage flux/sec variables (Ψ) can be written as:

$$\begin{aligned}
 \psi_q &= -X_{ls} i_q + \psi_{mq}, \\
 \psi_d &= -X_{ls} i_d + \psi_{md}, \\
 \psi_o &= -X_{ls} i_o, \\
 \psi_{aq} &= X_{laq} i_{aq} + \psi_{mq}, \\
 \psi_f &= X_{lf} i_f + \psi_{md}, \\
 \psi_{ad} &= X_{lad} i_{ad} + \psi_{md},
 \end{aligned} \tag{2}$$

where: X_{ls} , X_{laq} , X_{lad} , X_{lf} are the stator winding leakage reactance, q-axis and d-axis damping winding and the field winding leakage reactance respectively.

Ψ_{mq} and Ψ_{md} are the q-axis and d-axis magnetizing fluxes per second which are also the q-axis and d-axis magnetizing fluxes/second (magnetizing voltages)

If magnetic saturation is not considered it can be written:

$$\begin{aligned}
 \psi_{mq} &= X_{mq} i_{mq}, \\
 \psi_{md} &= X_{md} i_{md},
 \end{aligned} \tag{3}$$

where X_{mq} and X_{md} are the non-saturated q-axis and d-axis magnetizing reactance while i_{mq} and i_{md} are the

q-axis and d-axis magnetizing currents.

$$\begin{aligned} i_{mq} &= -i_q + i_{aq}, \\ i_{md} &= -i_d + i_f + i_{ad}. \end{aligned} \quad (4)$$

Using equations (2) and (4) it is possible to write:

$$\begin{aligned} \psi_q &= -X_q i_q + X_{mq} i_{aq}, \\ \psi_d &= -X_d i_d + X_{md} i_{ad}, \\ X_q &= X_{\ell s} + X_{mq}, \\ X_d &= X_{\ell s} + X_{md}, \end{aligned} \quad (5)$$

X_q , X_d are non-saturated synchronous reactance. Notice that all the rotor machine variables and parameters are referred to the stator winding.

3 SATURATION AFFECTING MACHINE STEADY-STATE VARIABLES

Utilities use to use the non-saturated and the saturated values of the d-axis and q-axis synchronous reactance to perform electrical system dynamic studies and use to ask to synchronous machine manufacturers for the non-saturated and saturated values of the d-axis and q-axis synchronous reactance. That is the same as to provide the non-saturated and saturated values of the d-axis and q-axis magnetizing reactance because leakage reactance is considered constant and non-saturated.

The non-saturated values of X_{md} and X_{mq} are the slopes of the air-gap lines in the (Ψ_{m_i}, i_{md}) and (Ψ_{m_q}, i_{mq}) magnetizing curves, respectively, as shown in the figure 2.

The saturated value of X_d is the inverse of the short-circuit ratio. The saturated d-axis magnetizing reactance can be calculated as $X_{mds} = X_d - X_{\ell s}$.

The short-circuit ratio is the ratio between the no-load field current at rated voltage and frequency and the field current necessary to have the short-circuit rated current at rated frequency in the short-circuited machine armature winding.

The saturated value of X_q is taken normally as 95% of the non-saturated value for large hydrogenerators and the saturated q-axis magnetizing reactance can be calculated as $X_{mq_s} = X_q - X_{\ell s}$.

Using the dynamic mathematical model provided in [5], constituted by the equations (1) to (5), it can calculate the values of the several variables involving the machine using magnetizing reactance X_{md} and also, X_d and X_q

as shown in [5] and in the equations (6).

$$\begin{aligned} |\dot{V}_a| &= \frac{V}{\sqrt{3}}, \\ \text{angle } \dot{V}_a &= 0 \text{ (reference)}, \\ |\dot{I}_a| &= \frac{S}{3 |\dot{V}_a|}, \\ \phi &= \text{angle } \dot{I}_a = \cos^{-1} \text{ (power factor)} \\ \dot{E}_a &= \dot{V}_a + (r_s + j X_q) \dot{I}_a = |\dot{E}_a| \text{ (angle } \delta), \\ I_d &= \sqrt{2} I_a \text{sen}(\phi + \delta), \\ E_f &= \sqrt{2} |\dot{E}_a| + (X_d - X_q) I_d, \\ I_f &= \frac{E_f}{X_{md}}, \end{aligned} \quad (6)$$

where: \dot{V}_a and V are respectively the phase armature voltage phasor and the line to line armature voltage (rms), \dot{I}_a is the armature current phasor, S is the apparent power (VA), I_f is the field current and I_d is the peak d-axis armature current

Using these equations it is possible to plot the machine V curve which is the curve of $|\dot{I}_a|$ against I_f for a given real power and variable power factor. These calculations were done for two different cases using the machine example data presented in the appendix.

In the **case 1** the non-saturated magnetizing reactance X_{md} and X_{mq} are used in the equations (6) and in the **case 2** the saturated values X_{mds} and X_{mq_s} are used in the equations (6).

Figure 1 shows the V curves for the 2 cases above and for the machine rated real power ($P = 1$ pu). It is possible to see that to get the same stator winding current (armature current) it is necessary to increase the field current about 15% when machine is saturated (in the sense of using saturated values of the reactance X_{mds} and X_{mq_s} to represent the saturation effects). It can be seen also that the curves are almost parallel, mainly in the inductive load region.

Table 1 shows, for the **case 1**, the values of the steady-state field current (I_f) when the armature voltage is $V = 1$ pu for three different values of the apparent power S ($S = 1.00$ pu, $S = 1.10$ pu and $S = 1.15$ pu) and machine rated power factor.

Table 2 shows the same values for the **case 2** where the saturation effect is included by considering X_{mds} and X_{mq_s} .

It can be noticed that the field current in the **case 2** (sat-

urated in the sense of using saturated magnetizing reactance) is about 9% larger than the field current shown in **case 1** (non-saturated).

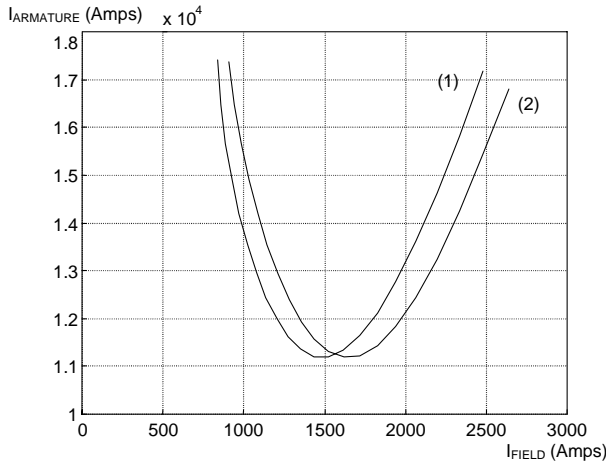


Figure 1: V curves for cases 1 and 2 (real power = 1.0 pu).

Table 1: Field current the case 1.

S (pu)	1.00	1.10	1.15
I_f (A)	1886	1976	2021

Table 2: Field current for the case 2.

S (pu)	1.00	1.10	1.15
I_f (A)	2059	2149	2194

4 SATURATION MODEL USING D-AXIS AND Q-AXIS MAGNETIZING CURVES

In this item a synchronous machine dynamic mathematical model is developed to included the saturation using the equations (1) to (5) and also the machine d-axis and q-axis magnetizing curves.

As it can be seen in the equations (1) and (2) the terms $p\Psi_q$ and $p\Psi_d$ transform themselves in $p\Psi_{mq}$ and $p\Psi_{md}$, respectively when the saturation in the air is neglected. To calculate them it is necessary to have the d-axis and q-axis magnetizing curves in a mathematical form.

Those curves can be provided by the machine manufacturer. The machine manufacturer can construct them in the machine design time or in its final tests according to the IEEE Standard [6]. A mathematical representation

through hyperbolic functions is used in this paper for the machine example.

The curves for the machine used in this paper (appendix) are shown in figure 2 where Ψ_m and I_m are the magnetizing flux/s and magnetizing current respectively.

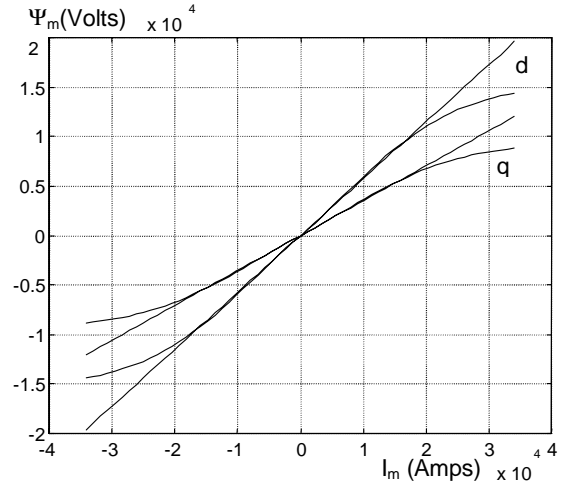


Figure 2: d-axis and q-axis magnetization curves.

In this paper unbalanced studies are not considered, so substituting equations (2) in (1), eliminating the zero sequence equation, and using the hyperbolic representation of (Ψ_{md}, i_{md}) and (Ψ_{mq}, i_{mq}) curves (appendix), it can be written:

$$\begin{aligned}
 p \Psi_{mq} &= \frac{d\Psi_{mq}}{di_{mq}} \frac{di_{mq}}{dt}, \\
 p \Psi_{md} &= \frac{d\Psi_{md}}{di_{md}} \frac{di_{md}}{dt}, \\
 p i_{mq} &= -p i_q + p i_{aq}, \\
 p i_{md} &= -p i_d + p i_f + p i_{ad}, \\
 f_c &= \frac{1}{X_{\ell s}} \frac{d\Psi_{mq}}{di_{mq}}, \\
 f_d &= \frac{1}{X_{\ell s}} \frac{d\Psi_{md}}{di_{md}}, \\
 f_{aq} &= \frac{1}{X_{\ell aq}} \frac{d\Psi_{mq}}{di_{mq}}, \\
 f_q &= \frac{1}{X_{\ell f}} \frac{d\Psi_{md}}{di_{md}}, \\
 f_{ad} &= \frac{1}{X_{\ell ad}} \frac{d\Psi_{md}}{di_{md}}.
 \end{aligned} \tag{7}$$

It is possible, after some simple algebraic calculations, to compact the six first equations (1) including the equations (7) in one matrix equation as below:

$$Mp\dot{\underline{i}} = \omega_b A \underline{v} - \omega_b B \dot{\underline{i}} - \omega_r \underline{\Psi}_m,$$

where:

$$\begin{aligned} \dot{\underline{i}} &= [i_q \ i_d \ i_{aq} \ i_f \ i_{ad}]^T, \\ \underline{v} &= [v_q \ v_d \ 0 \ i_f \ 0]^T, \\ \underline{\Psi}_m &= \left[\frac{\Psi_{md}}{X_{\ell s}} \quad -\frac{\Psi_{mq}}{X_{\ell s}} \quad 0 \quad 0 \quad 0 \right]^T, \\ M &= \begin{bmatrix} 1 + f_q & 0 & -f_q & 0 & 0 \\ 0 & 1 + f_d & 0 & -f_d & -f_d \\ f_{aq} & 0 & 1 - f_{aq} & 0 & 0 \\ 0 & f_c & 0 & 1 - f_c & f_c \\ 0 & f_{ad} & 0 & f_{ad} & 1 - f_{ad} \end{bmatrix}, \\ A &= \begin{bmatrix} -\frac{1}{X_{\ell s}} & -\frac{1}{X_{\ell s}} & 0 & \frac{1}{X_{\ell f}} & 0 \end{bmatrix}, \\ B &= \begin{bmatrix} \frac{r_s}{X_{\ell s}} & \omega_r & 0 & 0 & 0 \\ -\omega_r & \frac{r_s}{X_{\ell s}} & 0 & 0 & 0 \\ 0 & 0 & \frac{r_{aq}}{X_{\ell aq}} & 0 & 0 \\ 0 & 0 & 0 & \frac{r_c}{X_{\ell f}} & 0 \\ 0 & 0 & 0 & 0 & \frac{r_{ad}}{X_{\ell ad}} \end{bmatrix}. \end{aligned} \quad (8)$$

The values of the factors $f_q, f_d, f_{aq}, f_f, f_{ad}$ and the fluxes Ψ_{md} and Ψ_{mq} are calculated at each step of the differential equations numerical integration using the d-axis and q-axis magnetization curves (Ψ_{md}, i_{md}) and (Ψ_{mq}, i_{mq}) seen in the figure 2 and which algebraic equations are in the appendix.

5 SIMULATION RESULTS USING THE PRESENTED MATHEMATICAL MODEL

The mathematical model represented by the equations (1) to (5) is a linear dynamic model so that it is possible to derive a steady-state model from it simply making the derivative of the fluxes equal to zero and the algebraic complex equations (6) can be found [5].

Due to the non-linear character of the equations (7) and (8) the presented mathematical model can not be worked to find algebraic equations to represent the steady-state operation. The steady-state must be reached by solving the differential equations and waiting for the end of the transient state.

So to get the V curve using this model it is necessary to solve the differential equations (7) and (8), for each field current or field voltage, and wait for the steady-state to find the armature current.

Figure 3 shows the V curves for the 3 cases studied in this paper: curve 1 corresponds to the case 1 where the non-saturated reactance X_{md} and X_{mq} were used with the linear model, curve 2 corresponds to the case 2 where the saturated reactance X_{mds} and X_{mqs} were used with the linear model and curve 3 corresponds to the case 3 where the non-linear model presented in this paper that takes into account the machine magnetizing curves were used. The real power in this case is the rated power.

For each armature current value there are different values of the generator excitation current. For the armature rated current (12450 A, rated power factor) it

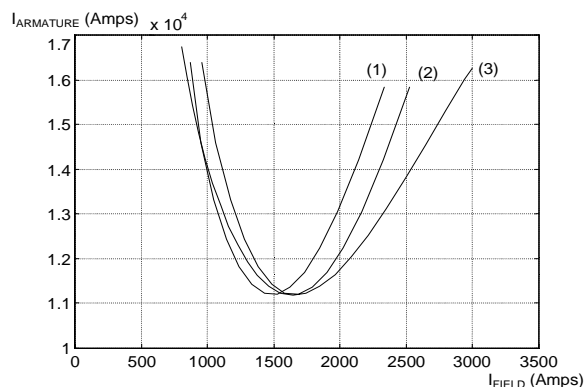


Figure 3: V curves for cases 1, 2 and 3 (real power = 1.0 pu).

has three different excitation currents, depending on the way the magnetic saturation is considered. For the way before named as 1 the excitation current is 1886 A, for the way named 2 it is 2059 A and for the third way it is 2184 A.

The same table shown before is shown now in table 3, for the new model. In this case a dynamic simulation was run to find the steady-state operating point.

Table 3: Field current for the new model.

S (pu)	1.00	1.10	1.15
I_f (A)	2184	2280	2329

It can be seen that field current is about 15% larger than the field current of the non-saturated case and about 6% larger than the field current of the case 2 where it was used saturated reactance.

6 EXPERIMENTAL RESULT AND COMPARISONS

Measurement carried out in the power plant where the generator is included, during the starting tests, had shown the excitation current of 2291 A for rated operation condition.

The errors can be calculated for the same operating conditions shown in the V curves of figure 3:

$$\begin{aligned}\varepsilon_1 &= \left(\frac{2291 - 1886}{2291} \right) \times 100\% = 17,76\% \\ \varepsilon_2 &= \left(\frac{2291 - 2059}{2291} \right) \times 100\% = 10,13\% \\ \varepsilon_3 &= \left(\frac{2291 - 2184}{2291} \right) \times 100\% = 4,23\%\end{aligned}\quad (9)$$

The experimental result shows that the presented non-linear model give a more accurate field current compared with the field current got from the linear model using non-saturated reactance or saturated reactance.

7 CONCLUSIONS

The linear model shown in the equations (1) to (5), with non-saturated or saturated reactance, despite to be frequently used by the engineers for steady-state and dynamic calculations, is not accurate. The errors in the steady-state field current are very high as it can be seen (items 5 and 6 (equations 8)).

The non-linear model presented in this paper, despite to spend more computational time to give the results, is more accurate to be used in electrical power system calculations.

ACKNOWLEDGMENT

Special thanks to Brazilian Research Council (CNPq) and São Paulo Research Foundation (FAPESP) for fund the authors Francisco Liszt Nunes Jr. and Sidney Osses Nunes.

REFERENCES

- G. Shaskshaft, and P. Henser, "Model of generator saturation for use in power system studies", IEE Proc., Vol. 126, No. 8, August 1979, pp. 759-763.
- R.G. Harley, D.J.N. Limebeer, and E. Chirricizzi, "Comparative study of saturation methods in synchronous machine models", IEE Proc., Vol. 127, Pt. B, No. 1, Jan 1980, pp. 1-7.

A.M. El-Serafi, and A.S. Abdallah, "Effect of saturation on steady-state stability of synchronous machines connected to an infinity bus system", IEEE Trans. On Energy Conversion, Vol. 6, No. 3, Sept. 1991, pp. 514-521.

F.P. De Mello, and L.N. Hannett, "Representation of saturation in synchronous machines", IEEE Trans. on Power Systems, Vol. PWRS-1, No. 4, Nov. 1986, pp. 8-18.

P.C. Krause, Analysis of Electric Machinery, McGraw Hill, 1986.

IEEE Std 115-1995, Guide: Test Procedures for Synchronous Machines, in IEEE Standards Collection Electric Machinery, Published by IEEE, 1997.

A APPENDIX

In this appendix the data of the hydrogenerator used as example in the paper are presented. This machine is ready to start operation in the Brazilian Electrical System.

Rated values:

345 MVA – 16 kV – 60 Hz – 0.9 pf – 80 poles.

Parameters:

$J = 28.8 \times 10^6 \text{ Js}^2$, $X_{\ell s} = 0.1144 \text{ } \Omega$, $X_{\ell f} = 0.0916 \text{ } \Omega$, $X_{\ell ad} = 0.1175 \text{ } \Omega$, $X_{\ell aq} = 0.0787 \text{ } \Omega$, $X_{md} = 0.5747 \text{ } \Omega$, $X_{mq} = 0.3524 \text{ } \Omega$, $r_s(75^\circ\text{C}) = 0.00181 \text{ } \Omega$, $r_f(75^\circ\text{C}) = 0.000247 \text{ } \Omega$, $r_{ad}(75^\circ\text{C}) = 0.00247 \text{ } \Omega$, $r_{aq}(75^\circ\text{C}) = 0.00533 \text{ } \Omega$, $X_{mds} = 0.5 \text{ } \Omega$, $X_{mqs} = 0.3312 \text{ } \Omega$. (all the rotor parameters are referred to the stator side).

Magnetizing curves presented in the figure 2 were provided by the manufacturer and can be represented by the following hyperbolic equations:

$$\begin{aligned}\psi_{md} &= c_d[\tanh(a_d i_{md}^2 \text{Sign}(i_{md}) + b_d i_{md}) + k_d i_{md}], \\ \psi_{mq} &= c_q[\tanh(a_q i_{mq}^2 \text{Sign}(i_{mq}) + b_q i_{mq}) + k_q i_{mq}],\end{aligned}$$

where:

$$\begin{aligned}c_d &= 1.0752 & a_d &= 0.1872 & b_d &= 0.8564 & k_d &= 0.0549, \\ c_q &= 0.6131 & a_q &= 0.2013 & b_q &= 0.9209 & k_q &= 0.0591.\end{aligned}$$